EPJ Web of Conferences **87**, 01003 (2015)
DOI: 10.1051/epjconf/20158701003

Influence of density fluctuations on the O–X mode conversion and on microwave propagation

A. Köhn[1,a], T. Williams[2], R. Vann[2], E. Holzhauer[1], J. Leddy[2], M. O'Brien[3], and M. Ramisch[1]

[1] *Institute of Interfacial Process Engineering and Plasma Technology, University of Stuttgart, Stuttgart, Germany*
[2] *York Plasma Institute, Department of Physics, University of York, York, U.K.*
[3] *CCFE, Culham Science Centre, Abingdon, Oxon, OX14 3DB, UK*

Abstract. Full-wave simulations are performed in order to investigate the interaction of plasma density perturbations and microwaves. The perturbations are divided into two cases: A single blob-like structure and a fully turbulent density profile. The resulting scattering of a microwave beam and the effect on the O–X mode conversion are presented for both cases. Quantitative analyses are performed as a function of the average size and position of the perturbations. The usage of spatial coordinates normalized to the vacuum wavelength of the microwave allows to easily adopt the results to a specific problem.

1 Introduction

Electromagnetic waves in the microwave regime are commonly used to both heat plasmas and diagnose them. If the plasma frequency exceeds the frequency of the corresponding microwave, the plasma is referred to as *overdense* and becomes inaccessible for waves of this frequency. One way to overcome this limitation is to use *electron Bernstein waves* [1] (EBWs): they are of electrostatic nature and have no high-density cut-off. The EBWs can be coupled to electromagnetic waves at the plasma boundary. Since they are very well absorbed at the electron cyclotron resonance layer and its harmonics, the EBWs can, on the one hand, be used for transferring energy to the plasma by coupling them to injected electromagnetic waves. On the other hand, EBWs are also generated by thermal fluctuations inside the plasma. Subsequent coupling to electromagnetic waves at the plasma boundary and detection of these waves allows them to be used as a diagnostics.

One possible coupling process is the so-called *O-X-B mode conversion*: an injected O-mode is converted to an X-mode in the vicinity of the O-mode cut-off layer. The X-mode then propagates outwards to the upper-hybrid resonance layer, where it is converted to a backwards propagating EBW. The reverse process can be used for emission diagnostics. The efficiency of the whole coupling process depends strongly on the efficiency of the O–X conversion, which, itself, depends on the injection angle with respect to the background magnetic field $\mathbf{B}_0$. The sensitivity on the angle is given by the normalized density gradient length $k_0 L_n = k_0 n_e / |\nabla n_e|$ (with k_0 the vacuum wave number of the electromagnetic wave and n_e the plasma density) at the conversion layer: The steeper the profile is, i.e. the smaller the value of $k_0 L_n$ is, the less sensitive is the conversion efficiency on angular mismatch.

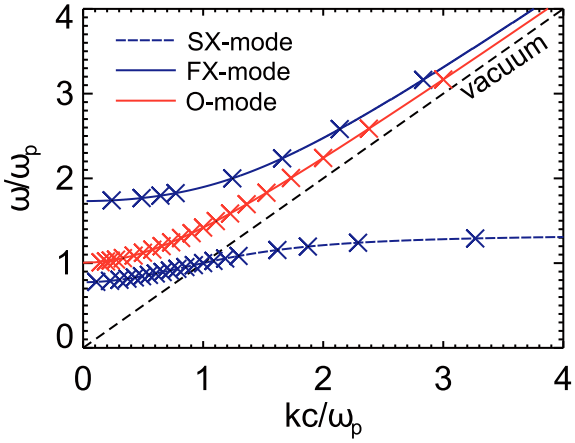

Figure 1. Comparison of the dispersion relation, normalized to the electron plasma frequency, of the O- and X-mode as obtained from full-wave simulation with IPF-FDMC (crosses) and from cold plasma theory (different colored lines).

Strong gradients at the plasma boundary can drive turbulence, which leads to perturbations in the plasma density. These perturbations can significantly distort a traversing microwave beam. Since the O–X mode conversion layer is usually located at the plasma boundary, the perturbations can result in a severe reduction of the coupling efficiency of the O-mode to the X-mode and, thus, to the EBW.

Full-wave simulations are performed to investigate and quantify the influence of density perturbations on this coupling process and on traversing microwaves in general. First, the deformation of a propagating microwave beam

[a] e-mail: koehn@igvp.uni-stuttgart.de

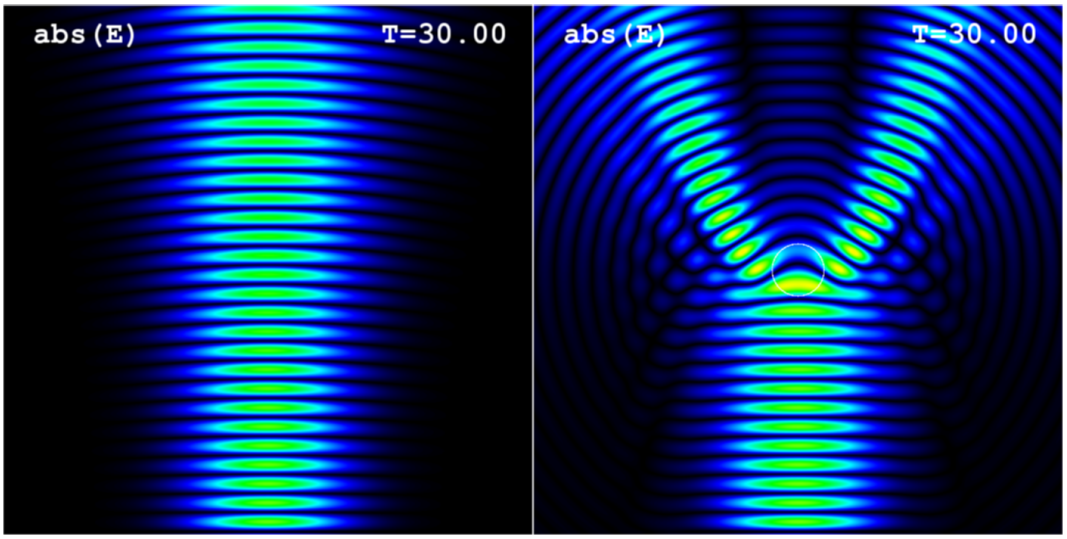

Figure 2. Absolute value of the wave electric field of a microwave beam propagating in vacuum (left) without a density perturbation and (right) with a blob-like perturbation elongated perpendicular to the simulation plane. The emitting antenna is located at the bottom. The microwave beam is of Gaussian shape and has a size at the waist of $w = 2 \cdot \lambda_0$.

by a single Gaussian-shaped density structure, similar to a *blob* or a *filament* [2], is presented and discussed as a function of the absolute density value, of the spatial size and of the position of the perturbation. The investigations are then extended to the influence on the O–X coupling process. Finally, broadband density fluctuations are considered, generated with a Hasegawa-Wakatani drift-wave turbulence model within the BOUT++ framework [3].

The simulations are performed with the 2D full-wave code IPF-FDMC [4]. The scattering process of microwaves at the blob-like perturbations is, in addition, analyzed with the 3D full-wave code EMIT-3D [5]. Excellent agreement is found for geometries, which are basically two dimensional in nature.

2 The full-wave code IPF-FDMC

The full-wave code IPF-FDMC is a finite-difference time-domain (FDTD) code, which simulates wave propagation in a cold magnetized plasma. Maxwell's equations are solved together with an equation for the current density $\mathbf{J}$, which is derived from the fluid equation of motion for the electrons. The equations are as follows:

$$\frac{\partial \mathbf{B}}{\partial t} = -\nabla \times \mathbf{E} \quad (1)$$

$$\frac{\partial \mathbf{E}}{\partial t} = c^2 \nabla \times \mathbf{B} - \mathbf{J}/\epsilon_0 \quad (2)$$

$$\frac{\partial \mathbf{J}}{\partial t} = \epsilon_0 \omega_{pe}^2 - \omega_{ce} \mathbf{J} \times \hat{\mathbf{B}}_0 - \nu \mathbf{J}, \quad (3)$$

with ω_{pe} the electron plasma frequency, ω_{ce} the electron cyclotron frequency, $\hat{\mathbf{B}}_0$ the unit vector into the direction of the magnetic field and ν the electron collision frequency. Based on the FDTD method (see e.g. [6]), the differential equations are solved by replacing the spatial derivatives with finite differences. Plasma density and background magnetic field profiles of arbitrary shape can be treated on a 2D grid. The code has been used previously to study the O–X–B mode conversion process in detail [7, 8] and to investigate microwave heating scenarios [9] .

The code allows for spatial variations of the background plasma parameters in two dimensions. By introducing a fixed parallel wavenumber in the third dimension, microwave beams with a fixed angle of the antenna beam are realized since the parallel wavenumber is constant (Snell's law). Thus, the O–X conversion can be treated in a 2D computational grid with the magnetic field pointing outwards of it.

To check the validity of the code, the dispersion relation of the O- and X-mode has been obtained from it and benchmarked against cold plasma theory. As one can see from Fig. 1, excellent agreement is found.

3 The influence of a single blob

The interaction of microwaves with single Gaussian-shaped density structures is investigated first. This problem has the advantage that it is easy to implement but still of physical importance, since these perturbations are similar to blobs. Blobs are perturbations in the plasma pressure elongated along a magnetic field line. They appear at the plasma boundary in both, tokamaks and stellarators, and are thought to be responsible for a significant fraction of transport losses [2].

In the simulations, the shape of the blob-like structure is defined by the following equation:

$$\tilde{n}_\mathrm{e} = \tilde{n}_\mathrm{e,peak} \exp\left(-\frac{r^2}{w^2}\right). \quad (4)$$

As can be seen, the perturbation is characterized by its width w, its peak density $\tilde{n}_\mathrm{e,peak}$ and its position r with respect to the center of the microwave beam. Such a single

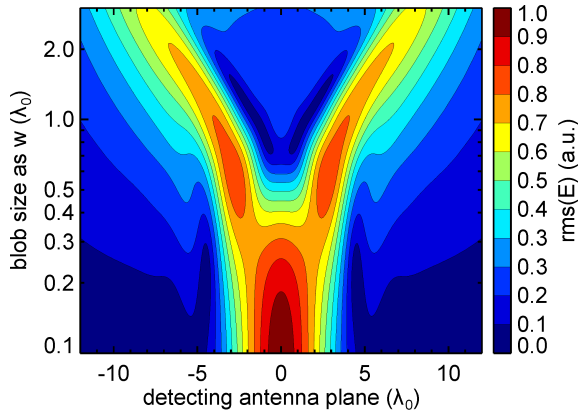

Figure 3. Contour plot of the spatial distribution of E_{rms} in the detecting antenna plane as a function of the coordinate along the antenna and of the size of the blob-like perturbation given by its width w (cf. Eq. 3). Note that the y-axis has a logarithmic scale.

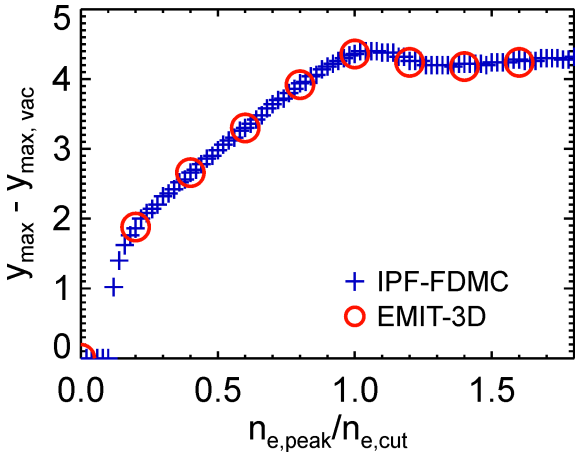

Figure 4. The position of maximum emission at the detector antenna as a function of the peak density of the blob-like perturbation. Crosses are from the 2D code IPF-FDMC, circles are from the 3D code EMIT-3D.

blob-like structure is added to an otherwise unperturbed background profile.

First, the interaction with a traversing microwave beam is analyzed followed by the influence on the O–X mode conversion process.

3.1 The impact on a traversing microwave beam

In this scenario, a microwave beam with a Gaussian amplitude distribution is injected onto the computational grid from the bottom. The beam waist is set to a size of $w_0 = 2\lambda_0$ and the wave is considered as being linearly polarized. The background is set to vacuum (without a magnetic field) in order to elucidate the scattering process at the blob-like structure. With the structure being elongated perpendicular to the computational grid (parallel to the wave polarization), this corresponds to the scattering process of an O-mode.

To illustrate the effect of a single blob on a microwave beam, Fig. 2 shows a snapshot of the wave electric field of a microwave beam propagating in vacuum on the left-hand side and, on the right-hand side, for the same geometry but with a blob, as described by Eq. 3, added to it. The snapshot is taken after 30 oscillation periods. At this time, the steady state solution is achieved. Absorbers are placed around the computational grid. To have the highest impact on the microwave beam, the blob was positioned at the beam axis.

Although the peak density of the blob is under-dense with $\tilde{n}_{\mathrm{e,peak}} = 0.8 \cdot n_{\mathrm{e,cut}}$ (the width of the blob was set to $w = 1 \cdot \lambda_0$), the difference of the wave electric fields of both cases is obvious.

To investigate this interaction process in a more quantitative way, a receiving antenna is placed at the top of the simulation grid. This antenna is elongated along the whole width of the grid. It detects the rms-value of the wave electric field.

The signal detected is shown in Fig. 3 as a function of the size of the blob-like structure, given by its width w. For this scan, the perturbation was placed in vacuum and set to have a density of $\tilde{n}_{\mathrm{e,peak}} = 0.8 \cdot n_{\mathrm{e,cut}}$. Only weak distortion is found for small perturbations with $w < \lambda_0/3$. Above this value, the influence on the microwave is significant, best expressed by the position of maximum emission, which is no longer located at the center of the detector antenna. It can also be seen that for very large perturbations, the distortion is found to decrease again. Perturbations having a size on the order of the vacuum wavelength result in the largest deterioration of the microwave beam.

Obviously, the density of the perturbation plays an important role, too. To quantify its influence on the microwave beam, the position of maximum emission in the plane of the receiving antenna is shown in Fig. 4 as a function of the perturbation's peak density $\tilde{n}_{\mathrm{e,peak}}$. The width of the perturbation was kept constant at a value of $w = 1\lambda_0$ and it was positioned at the center of the grid for this scan. For low densities of $\tilde{n}_{\mathrm{e,peak}} \leq 0.1 \cdot n_{\mathrm{e,cut}}$, no shift in the position of maximum emission is found. A shift strongly increasing with the peak density is found up to a value of $\tilde{n}_{\mathrm{e,peak}} \leq 0.2 \cdot n_{\mathrm{e,cut}}$. For larger values, the slope in the shift of the position of maximum emission is slightly reduced.

In addition, Fig. 4 does not only show results obtained with the code IPF-FDMC, described in Sec. 2. It allows to compare with results obtained from the 3D code EMIT-3D. As can be clearly seen, perfect agreement is found between the two codes, showing that the scattering process is basically two dimensional in nature.

The same degree of agreement is found for the scan of the perturbation's size, as described by Fig. 3, and for the dependence of the distortion of the microwave beam on the perturbation's position with respect to the beam axis, not shown here. These comparisons are discussed in detail in Ref. [5].

3.2 The impact on the O–X conversion

To investigate the influence of a blob on the O–X mode conversion process, a density gradient needs to be intro-

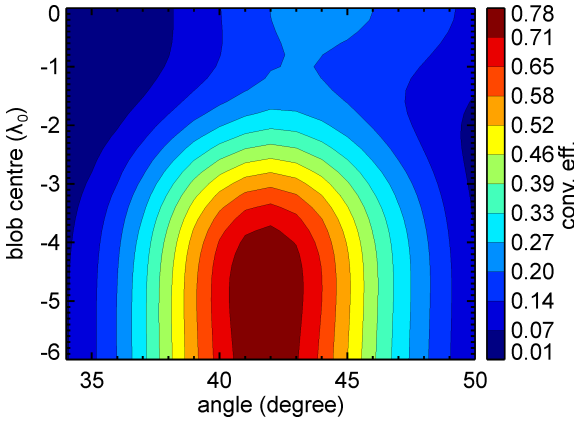

Figure 5. Contour plot of the O–X mode conversion efficiency as a function of the injection angle and of the position of the blob-like perturbation, moving along the density layer with a value of $n_e = 0.6 \cdot n_{\mathrm{e,cut}}$. Simulations were carried out with IPF-FDMC in a poloidal cross section.

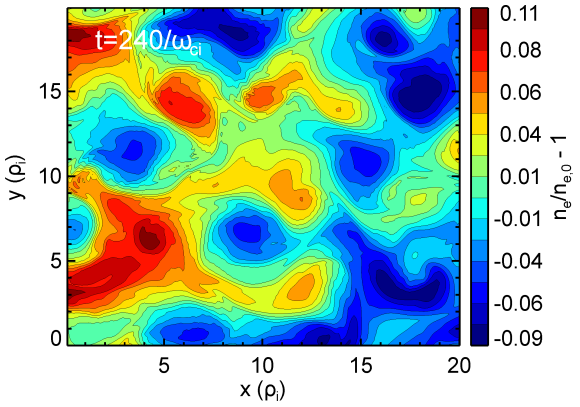

Figure 6. Contour plot of the relative density variation of one time slice generated by a Hasegawa-Wakatani turbulence model within the BOUT++ framework. The spatial coordinates are normalized to the ion Larmor radius ρ_i and the time is normalized to the ion cyclotron frequency ω_{ci}.

duced together with a background magnetic field. A linear increasing profile is chosen with a normalized density gradient of $k_0 L_n = 30$ (corresponding to the one used in Ref. [4]). The magnetic field is set to a constant value of $Y = \omega_{ce}/\omega_0 = 0.8$. The blob-like perturbation is described by Eq. 3 with default values of $w = 1 \cdot \lambda_0$ and $\tilde{n}_{\mathrm{e,peak}} = 2 \cdot n_{\mathrm{e,background}}$.

Similar to the analyses presented in Ref. [4], separate simulations in a toroidal and a poloidal plane are carried out. In the toroidal geometry, the magnetic field points into one of the directions of the 2D computational grid, whereas in the poloidal geometry the magnetic field points outwards of the computational grid. Hence, the blob-like structure is elongated along the computational plane in the toroidal case and perpendicular to it in the poloidal case. Toroidal and poloidal curvature of the plasma is neglected. As has been shown in Ref. [4], the curvature of the mode conversion layer can be compensated for by appropriate shaping of the microwave beam leading to same results as without plasma curvature. Therefore, the assumption of a straight conversion layer is justified.

In this paper, only the case of the poloidal plane will be discussed, corresponding to the case discussed in Sec. 3.1. The blob-like perturbation is expected to lead to a stronger deterioration in this case due to the direction of its density gradient with respect to the direction of propagation of the microwave beam.

Figure 5 shows the O–X conversion efficiency as a function of the injection angle and of the position of the perturbation with respect to the center of the microwave beam. If the blob is positioned far away from the center of the microwave beam, the angular dependence of the conversion efficiency exhibits a Gaussian behavior, as expected (see Ref. [4]). As soon as the center of the density perturbation is within the beam width of the microwave beam, a reduction of the conversion efficiency sets in. In the worst case, where the perturbation is located at the center of the microwave beam, the efficiency drops by a factor of approximately 3.

Keeping the results presented in Sec. 3.1 in mind, this strong deterioration is not surprising: A blob-like perturbation of the size considered was shown to have the largest influence on a traversing microwave (Fig. 3). It leads to strong scattering. For the O–X conversion this means a lot of new angular components are generated reducing the O–X conversion efficiency. Hence, the case presented in Fig. 5, represents a worst case scenario allowing to estimate the maximum deterioration of a blob-like structure on the O–X conversion process.

4 The influence of a realistic turbulent density profile

To simulate the influence of plasma density turbulence on propagating microwaves and on the O–X mode conversion process, it is necessary to have a large set of turbulent density profiles: Only by averaging over an ensemble of profiles, the results are statistically relevant. A Hasegawa-Wakatani drift-wave turbulence model is used to generate such a set of profiles within the BOUT++ framework [3]. These are 2D simulations with the background magnetic field pointing outwards of the simulation domain (corresponding to the poloidal plane introduced in Sec. 3.2). Various amplitudes of turbulence can be realized. Here, the relative fluctuation amplitude is set to a value of 10 %.

A set of density profiles is obtained by simply extracting multiple time slices from the simulations. One of these slices is shown in Fig. 6. Note that in the simulations, the background density must be added to these relative fluctuations. To investigate the scattering process, here, a density of $n_{\mathrm{e,background}} = 0.5 \cdot n_{\mathrm{e,cut}}$ was chosen.

The geometry of the simulations of the microwave-plasma interaction is such that the microwave propagates first in a region of unperturbed plasma. Then, it passes a region of turbulence taken as a cut from the turbulent density profile like the one shown in Fig. 6. This cut with

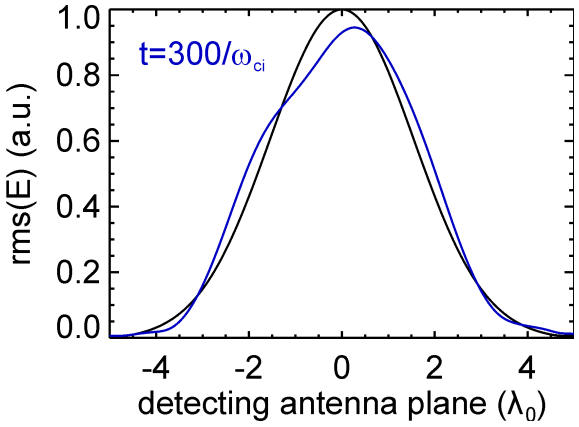

Figure 7. E_{rms} at the receiving antenna of a microwave which has passed a region of turbulence (blue line) and, as comparison, without having passed a region of turbulence (black line).

a length of $2 \cdot \lambda_0$ is convoluted with a spatial windowing function smoothing its edges in front of both the transmitting and the receiving antenna, which are placed in a region of unperturbed plasma. As in Sec. 3, the rms-value of the wave electric field is measured. By varying the scaling between the Larmor radius ρ_i and λ_0, the average spatial size of the turbulent structures (with respect to λ_0) can be varied.

Figure 7 shows the rms-value of the wave electric field detected at the receiving antenna, i.e. after the microwave has passed the region of turbulence. For comparison, the signal of a microwave propagating in the same grid but without any density perturbations is also shown. The deformation of the microwave beam is noticeable although not severe for the parameters chosen here.

The number of ensembles to average over has been set to 100, meaning that 100 simulations need to be carried out for each set of parameters. To quantify the deformation of the microwave beam, the difference of the signal detected at the receiving antenna to the unperturbed case is calculated as the square of the difference at each spatial position at the antenna. These values are then summed up to have one number for each set of parameters.

Varying the average spatial size of the turbulence and performing the analysis just described it is found that the deformations of the microwave beam do not vary much if the perturbations' size is $3\lambda_0$ or larger. If, however, the size decreases below this value, the deformation strongly increases. The strongest deformation is, again, found for an average structure size corresponding approximately to the vacuum wavelength of the microwave.

To simulate the influence on the O–X mode conversion process, the turbulence needs to be added to a background density profile having a finite density gradient. Similar simulations have been carried out in a 1D geometry previously [10]. At present, these simulations are extended to a 2D poloidal geometry using the turbulence presented above. The results will be presented in a subsequent presentation.

5 Summary

The influence of density perturbations on propagating microwaves and on the O–X mode conversion process has been investigated using 2D full-wave simulations. First, the influence of a single blob-like perturbation has been analyzed. It was shown that a perturbation having a size on the order of the vacuum wavelength of the injected microwave has the largest influence. Even if the perturbation's density is a factor of 5 below the cut-off density it already has a significant influence. The scattering of the injected microwave at the blob-like perturbation has also been analyzed with a 3D full-wave code. Excellent agreement was found.

A set of fully turbulent plasma density profiles have been generated with a Hasegawa-Wakatani drift-wave model. To be statistically relevant, an ensemble of 100 density profiles has been treated for each set of parameters in the simulations. Again, the scattering of the microwave was found to be the largest if the average spatial size of the turbulent structures is on the order of the vacuum wavelength of the microwave. Simulations of the influence on the O–X mode conversion process are performed at the moment and will be presented in a future publication.

References

[1] H. P. Laqua, Plasma Phys. Control. Fusion **49**, R1 (2007)

[2] D. A. D'Ippolito *et al.*, Phys. Plasmas **18**, 060501 (2011)

[3] B Dudson *et al.*, Comp. Phys. Comm. **180**, 1467 (2009)

[4] A. Köhn *et al.*, Plasma Phys. Control. Fusion **50**, 085018 (2008)

[5] T. R. N. Williams *et al.*, Plasma Phys. Control. Fusion *accepted*

[6] A. Taflove and S. C. Hagness, *Computational Electrodynamics: the Finite-Difference Time-Domain Method* (Artech House Publishers, Boston, 2000)

[7] A. Köhn *et al.*, IEEE Trans. Plasma Sci. **36**, 1220 (2008)

[8] R. Bilato *et al.*, Nucl. Fusion **49**, 075020 (2009)

[9] A. Köhn *et al.*, Plasma Phys. Control. Fusion **52**, 035003 (2010)

[10] A. Köhn *et al.*, *38th EPS Conference on Plasma Phys.* (ECA 35G, P2.020, Strasbourg, 2011)